



Protecting America's Future

Y/DZ-2633

Casting to Geometrical Specification: Theory and Practice of Simulation Uncertainty and Sensitivity

A. J. Baker and Marcel A. Grubert
University of Tennessee, Knoxville, TN, 37996-2030

V. E. Lamberti
Technology Development
Applied Technologies Division

Issue Date: June, 2005

Submitted to
Metallurgical and Materials Transactions B

COPYRIGHT NOTICE

This document has been authored by a subcontractor of the U.S. Government under contract DE-AC05-00OR-22800. Accordingly, the U.S. Government retains a paid-up, nonexclusive, irrevocable, worldwide license to publish or reproduce the published form of this contribution, prepare derivative works, distribute copies to the public, and perform publicly and display publicly, or allow others to do so, for U.S. Government purposes.

Prepared by the
Y-12 National Security Complex
P.O. Box 2009, Oak Ridge, Tennessee 37831-8169
Managed by
BWXT Y-12, L.L.C.
for the
U.S. DEPARTMENT OF ENERGY
under contract DE-AC05-00OR22800

MANAGED BY
BWXT Y-12, L.L.C.
FOR THE UNITED STATES
DEPARTMENT OF ENERGY

UCN-13672 (11-03)

**Y-12
NATIONAL
SECURITY
COMPLEX**

DISCLAIMER

This report was prepared as an account of work sponsored by an agency of the United States Government. Neither the United States Government nor any agency thereof, nor any of their employees, makes any warranty, express or implied, or assumes any legal liability or responsibility for the accuracy, completeness, or usefulness of any information, apparatus, product, or process disclosed, or represents that its use would not infringe privately owned rights. Reference herein to any specific commercial product, process, or service by trade name, trademark, manufacturer, or otherwise, does not necessarily constitute or imply its endorsement, recommendation, or favoring by the United States Government or any agency thereof. The views and opinions of authors expressed herein do not necessarily state or reflect those of the United States Government or any agency thereof.

Casting to Geometrical Specification: Theory and Practice of Simulation Uncertainty and Sensitivity

A. J. Baker* and Marcel A. Grubert†
University of Tennessee, Knoxville, TN 37996-2030

V. E. Lamberti‡
Y-12 National Security Complex, Oak Ridge, TN 37831-8096

Computational prediction of the properties of cast objects can be substantially hindered by absence of truly accurate thermo-physical data for the materials and process conditions involved. Uncertainty analysis quantifies the impact on a simulation prediction of imprecise input data. Sensitivity analysis quantifies the susceptibility of simulation model output to input data uncertainty. The associated non-linear computational theory embedding uncertainty-sensitivity analysis within a fully coupled fluid-thermal-structural description of the casting process is developed. Numerical simulation of an axisymmetric casting model generates key data distributions characterizing the theory finite element implementation.

Nomenclature

c_p	=	specific heat
G	=	elastic shear modulus
h	=	enthalpy
k	=	thermal conductivity
L	=	latent heat
u	=	displacement
r	=	radial position
T	=	temperature difference
α	=	thermal expansion coefficient
ε	=	strain tensor
ϕ	=	metallurgical phase
λ	=	Lame parameter
ρ	=	density
σ	=	stress tensor

I. Introduction

The design criteria for as-cast metallurgical adequacy contains at least the following elements:

- casting to final shape tolerance
- segregation of minor components, porosity, inclusions
- crystal structure, with specific reference to brittleness and ductility
- residual stress, residual strain estimation

The ability to impact, estimate, and eventually exert *a priori* control of the casting process starts with mold design for quality filling but ultimately gets down to establishment of a dynamic mold cooling protocol.

* Prof., Engineering Science, Director UT CFD Laboratory, 316A Perkins Hall, University of Tennessee, Knoxville, TN 37996-2030, AIAA Associate Fellow.

† PhD Student, CFD Laboratory, 323 Perkins Hall, University of Tennessee, Knoxville, TN 37996-2030, AIAA student member.

‡ Chemistry and Chemical Engineering Department, Y-12, PO Box 2009, MS 8096, Oak Ridge, TN 37831-8096.

Numerous commercial software packages exhibit the capability to perform thermal, fluid, and stress calculations pertinent to metal casting. As with all such numerical modeling and simulation undertakings, accuracy of the terminal result is of paramount importance. A significant detractor to accurate prediction of the final shape, hence properties of cast objects, is the lack of accurate thermal, physical, and structural data for the materials present and the pertinent process conditions.

To estimate the impact of unreliable thermo-physics closure data on the validity of simulations, uncertainty analysis, either inverse or direct, and its close relative sensitivity analysis may be employed. Uncertainty analysis quantifies the impact on a simulation prediction of imprecise input data (*parametric* uncertainty) and the structure of the underlying model (*structural* uncertainty). Sensitivity analysis quantifies the susceptibility of simulation model output to input data uncertainty—that is, the evolutionary change of the prediction with respect to all input parameters, separately or in conjunction.

From a review of the recent literature^{1,2,3} and the results of a contractual technical study,⁴ conclusions pertinent to the casting simulation inverse-sensitivity issue indicate:

- mathematically, the optimal prediction of casting to a defined tolerance would utilize classical inverse sensitivity analysis;
- inverse sensitivity analysis is mathematically ill-posed, hence its stable utilization is subject to numerous practical implementation constraints;
- classical inverse sensitivity is viable only when using very accurate numerics for the thermal and displacement models associated with a simulation;
- specifically, “noise” in the data representing the input tolerance can totally destroy inverse sensitivity analysis stability; and
- sensitivity theory, focused on quantifying thermo-physics material properties uncertainties input to a simulation model, forms the mathematical foundation for both inverse and forward sensitivity analysis applications.

A computer-enabled casting simulation process involves generating an approximate solution to a set of non-linear partial differential equations (PDEs), closed with boundary conditions (BCs, with uncertainties $\pm \beta$), for the available thermo-physical data base (with uncertainties $\pm \delta$) via discrete numerics (with accuracy uncertainty $\pm \epsilon$). Initial conditions (ICs) are required to start the solution process. Figure 1 organizes the interplay of associated mathematics, physics, and thermo-physical data closure issues leading to the inverse, uncertainty, and sensitivity components of an analysis. The column of left boxes delineates the essence of solution approaches, each feeding the simulation identified as the central box. The right column of boxes identifies the key words associated with the resulting simulation.

The developed conclusion is that the lowest left and right boxes best describe the stable approach to simulation of dynamic mold cooling processes for optimal production.

II. Casting Uncertainty – Sensitivity Theory

Casting to shape $S = S(x,y,z,t)$, within a permissible variation dS , is the crux of the matter for production casting. Development of the mathematical definition for the time evolution of $S + dS$ during the in-mold cooling process is key to prediction of what is colloquially termed “shrinkage.” Assuming that no solidification occurs during mold fill, the technical requirement starts with the exothermic solidification process in the “mushy zone,” followed by a thermo-elastic displacement analysis during in-mold, eventually open-mold, cooldown with associated material properties dependencies on phase and temperature.

A. Thermal Displacement Theory

The mathematical formulation centers on the generic position vector $\mathbf{r}(\mathbf{x}, t)$ in the casting. During cooldown, associated with the temperature process dT , the structural analysis mathematical model must predict the change $d\mathbf{r}$ in the position vector. The ability to predict the evolution of $d\mathbf{r}$, mathematically expressed as the thermally induced displacement field $\mathbf{u}(\mathbf{x}, t)$, is subject to the uncertainties in all components of the mathematical model, as highlighted in Fig. 1. This, of course, generates the sensitivity analysis requirement developed herein.

Mathematically, the evolution of the displacement field $\mathbf{u}(\mathbf{x}, t)$ is the functional

$$\mathbf{u} = \mathbf{u}(\mathbf{x}, t, G, \lambda, \alpha, T(k, \rho, c_p, \phi, f, L)) \quad (1)$$

where (\mathbf{x}, t) is space-time, and G , λ and α are the elastic shear modulus, Lamé' parameter, and thermal expansion material properties embedded in the mechanical equilibrium conservation principle closed with the Hooke's law elastic constitutive model. The tensor field form is

$$\sigma_{ij} = \lambda \delta_{ij} \varepsilon_{kk} + 2G \varepsilon_{ij} - (3\lambda + 2G) \alpha T \delta_{ij} \quad (2)$$

where σ_{ij} and ε_{ij} are the stress and strain tensors, respectively, and T is temperature difference. The strain tensor kinematic correlation with the displacement field \mathbf{u} , assuming small displacements, is

$$\varepsilon_{ij} = \frac{1}{2} \left(\frac{\partial u_i}{\partial x_j} + \frac{\partial u_j}{\partial x_i} \right) \quad (3)$$

Returning to Eq. (1), the temperature field $T = T(\mathbf{x}, t, k, \rho, c_p, \phi, f, L)$ couples the prediction of displacement to the thermal history of the casting cooldown process. The temperature field is described mathematically by the energy conservation principle closed with the Fourier conduction model in the form

$$DE : \quad \rho \frac{\partial h}{\partial t} - \nabla \cdot k \nabla T - s = 0 \quad (4)$$

where $h = h(c_p, T)$ is enthalpy; ρ , c_p , and k are density, specific heat, and thermal conductivity material properties, respectively; and $s = s(L, T)$ is the placeholder for the exothermic solidification process for latent heat L . All material properties are dependent on metallurgical phase ϕ , and on T as well within each phase, and f signifies the mushy zone solidification model for handling L .

Equations (1)–(4) define parametrically the sensitivity of prediction of the displacement field during solidification to the material database with its intrinsic uncertainty properties. The elements of the associated sensitivity matrix are

$$\frac{\partial \mathbf{u}}{\partial (p_\alpha, T(p_\beta))} \quad (5)$$

The sensitivity of a displacement field prediction is the differential $\delta \mathbf{u}$ defined by the Taylor series

$$\begin{aligned} \delta \mathbf{u} &= \frac{\partial \mathbf{u}}{\partial p} \delta p + \frac{\partial \mathbf{u}}{\partial T} \delta T \\ &= \frac{\partial \mathbf{u}}{\partial p_\alpha} \delta p_\alpha + \frac{\partial \mathbf{u}}{\partial T} \frac{\partial T}{\partial p_\beta} \delta p_\beta \end{aligned} \quad (6)$$

the form of which segregates the elasticity model parameter uncertainties from the thermal data base uncertainties. The elements of these parameter sets are

$$\left. \begin{aligned} p &\Rightarrow p_\alpha = (G, \lambda, \alpha, T, \rho(\phi)) \\ & p_\beta = (k, \rho, c_p, L, \phi, f) \end{aligned} \right\} \quad (7)$$

An inverse sensitivity analysis defines $\delta \mathbf{u}$ and seeks determination of the sensitivities δp_α and δp_β that produce this desired state. The alternative, avoiding the inherent ill-posedness, is to execute an assortment of forward sensitivity problems—that is, compute δp_α and δp_β from first principles, hence determine a range for $\delta \mathbf{u}$. These well-posed problem statements are readily converted to computational syntax using established finite element (FE)

procedures.⁵ Via extremization of the FE approximate discrete construction of the Principle of Virtual Work,⁶ Eqs. (1)–(3) become the algebraic matrix equation system

$$\frac{\partial \Pi_e^h}{\partial \{\mathbf{U}\}_e} \Rightarrow [\text{STIFF}(\lambda, \mathbf{G})]\{\mathbf{U}\}_e - [\text{THERM}(\lambda, \mathbf{G}, \alpha)]_e \{T\}_e - \{\text{GRAV}(\rho, \mathbf{g})\} \quad (8)$$

The column matrix $\{\mathbf{U}\}$ is the displaced state distribution at the nodes of the FE mesh at any specific time. Functional dependence on material parameters is noted in Eq. (8), where $[\text{STIFF}(\cdot)]$ is the structural “stiffness matrix,” $[\text{THERM}(\cdot)]$ is the thermal expansion contribution, and $\{\text{GRAV}(\cdot)\}$ results from the gravity body force.

Several recent publications have focused strictly on sensitivity constructions for the energy principle, Eq. (4), specifically addressing the handling of temperature dependent specific heat and latent heat in the mushy zone.^{2,3} A precise examination of the construction confirms that the proposed handling of the enthalpy-temperature mix in Eq. (4) was mathematically inconsistent requiring an implementation approximation.

The elimination of the enthalpy crutch in Eq. (4), coupled with a consistent handling of temperature dependent specific heat, precisely eliminates this problem. The theory simply employs a Taylor series, for both c_p and k , leading to a cubically non-linear rearrangement of Eq. (4) to the form

$$DE: \quad \rho(a_c + b_c T + c_c T^2) \frac{\partial T}{\partial t} - \nabla \cdot (a_k + b_k T + c_k T^2) \nabla T - s(L) = 0 \quad (9)$$

The coefficient sets a , b , and c for c_p and k , subscripted “ c ” and “ k ” respectively, replace the sensitivity parameters “ c_p ” and “ k ” in Eq. (7) with an accurate (up to quadratic) delineation of the temperature dependence of these material properties. Further, this procedure admits separation of the latent heat handling from enthalpy and places its action as a heat source $s(L)$ dependent on latent heat.

B. Finite Element Implementation

The formulation of the FE algorithm for the non-linear energy principle, Eq. (9), follows standard practice.⁵ The functional form of the resultant algebraic equation system is

$$\begin{aligned} \frac{\partial \Pi^h}{\partial \{\mathbf{U}\}} &= S_e [[\text{MASS}(\rho, c_p(a, b, c))\{Q - \text{QN}\} - \Delta t \{b(L, \text{QR}, \text{QC})\} \\ &+ \Delta t [\text{DIFF}(k(a, b, c))]_e \{Q\}_0 + \Delta t [\text{BC}(\alpha, h)]\{Q\}] = \{0\} \end{aligned} \quad (10)$$

where $[\text{MASS}(\cdot)]$, containing the c_p temperature dependence, multiplies the nodal temperature change array $\{Q - \text{QN}\}$, over the time interval Δt , and $[\text{DIFF}(\cdot)]$ contains the resolved temperature dependence for conductivity multiplying the current nodal temperature array $\{Q\}$. The data matrix $\{b(\cdot)\}$ contains the implementation for latent heat in the mushy zone, for temperature range (QR, QC) over which it is defined to occur, and $\{\text{BC}(\cdot)\}$ is the placeholder for the radiation and/or convection BCs that may be applied.

With Eq. (10), precise expressions for the sensitivity matrix entries, $\partial T / \partial p_\beta$ in Eq. (6), can be made, which are themselves partial differential equations. Denoting a sensitivity matrix entry as $S_{p_\beta}(T)$, the definition is

$$S_{p_\beta}(T) \equiv \frac{\partial T}{\partial p_\beta} \Rightarrow \frac{\partial T}{\partial((a, b, c)c_p, k)} \quad (11)$$

Since temperature is the solution to Eq. (10), the PDE satisfied by the representative sensitivity matrix entry is derived as

$$\frac{\partial DE}{\partial p_\beta} = \frac{\partial}{\partial p_\beta} \left(\rho c_p \frac{\partial T}{\partial t} - \nabla \cdot k \nabla T - s \right) = 0 \quad (12)$$

Proceeding through the details, the PDE defining the evolution of the sensitivity matrix array is determined from Eq. (12) as

$$\mathcal{L}(S_\beta(T)) = \rho c_p \frac{\partial S_\beta(T)}{\partial t} - \nabla \cdot k \nabla S_\beta(T) + f_\beta \left(\frac{\partial p}{\partial p_\beta}, \frac{\partial c_p}{\partial p_\beta}, \frac{\partial s}{\partial p_\beta}, \frac{\partial k}{\partial p_\beta} \right) = 0 \quad (13)$$

which is readily recognized as the energy principle PDE with a new source term $f(\text{parametric sensitivity})$ entries identified in Eq. (6). Specific forms for the source term $f(\cdot)$, as a function of the precise character of temperature uncertainty in c_p and L , include:

- the level of c_p or k :

$$f_\beta(\cdot) = \rho \frac{\partial T}{\partial t}, \quad \text{or} \quad \nabla^2 T \quad (14)$$

- the slope of c_p or k versus temperature:

$$f_\beta(\cdot) = \rho T \frac{\partial T}{\partial t}, \quad \text{or} \quad T \nabla^2 T \quad (15)$$

- the curvature of c_p or k versus temperature:

$$f_\beta(\cdot) = \rho T^2 \frac{\partial T}{\partial t}, \quad \text{or} \quad T^2 \nabla^2 T \quad (16)$$

- the mushy zone latent heat model:

$$f_\beta(\cdot) = \frac{\partial S}{\partial p_\beta} = \frac{\partial S}{\partial f_s(\Delta t)} \quad (17)$$

It remains to couple the temperature sensitivity to the prediction of the displaced state, the $\partial \mathbf{u}^h / \partial T$ pre-multiplier in Eq. (6). Recalling the FE Virtual Work formulation, Eq. (8), the coupling matrix is [THERM(.)], hence the terminal sensitivity expression for displacement as a function of time and the temperature sensitivity of the material and model parameters is

$$\begin{aligned} S_{p,\beta}(\mathbf{u}^h) &\Rightarrow [\text{THERM}] \cdot \text{FE}(\mathcal{L}(S_\beta(T))) \\ &\Rightarrow S_e \left([\text{square matrix}]_e \cdot \{S_\beta^h(T(t))\}_e \right) \Rightarrow \{S_{p,\beta}(\mathbf{u}^h)\} \end{aligned} \quad (18)$$

where FE denotes the finite element solution of Eq. (13) over the time interval appropriate for a specific source term selection $f(\cdot)$.

The finite element implementation of the developed thermo-structural sensitivity theory is complete. The theory accepts non-linear temperature and phase dependence for c_p and k , phase dependence for density, and an exothermic formulation for the mushy zone solidification process over a definable temperature range. The resultant uncertainty-sensitivity simulation model predicts time-accurate evolution of temperature distributions coupled to quasi-static solutions for structural displacement at select time intervals.

III. Discussion and Results

Figure 2 illustrates the axisymmetric geometry for the problem class under consideration. Figure 3 presents a perspective of the Truchas code⁷ solution at $t = 300$ sec into mold cooldown, illustrating thermal simulation essence. The region of principal interest regarding thermal distortion is the cylindrical shell. Figure 3 confirms that vertical gradients therein are minimal, hence the theory implementation exercise was reduced to pure axisymmetric, wherein radial displacement is generated by hoop stress.

The implementation of the FE sensitivity theory employed Matlab,⁸ utilizing the UT CFD Lab academic toolbox. The appendix presents the associated linear basis FE algorithm template, implemented for assumed quadratic temperature dependence for specific heat, c_p , and conductivity, k . Figure 4 presents the model problem geometry, constituted of graphite cylinders enclosing the casting. Both graphite cylindrical surfaces were subjected to a combined convection and radiation boundary condition. The initial condition is mold and molten alloy at 1450 K. The thermo-physical property database, Table 1, confirms that only the alpha phase of the alloy exhibits temperature dependence.

For orientation, Figure 5 summarizes the FE algorithm prediction of radial displacement and temperature distributions, graphed in comparison to liquid-phase-solid regions, for simulation elapsed times $t = 1, 51, \text{ and } 501$ sec. The domain $0.1 \leq r \leq 0.2$ m is spanned by a 100 element uniform discretization, the simulation is time-accurate via the trapezoidal time integration rule, and the alpha phase is encased by solidified shells at $t = 501$ sec. The entire mold-casting assembly undergoes a radial displacement distribution as a function of time, and the various temperature distributions confirm surface cooling. The extremum radial displacement range for the solidified casting is $0.0002 \leq \Delta r \leq 0.00045$ m. This base simulation was repeatedly re-executed, selectively solving in the process the developed sensitivity FE algorithms for alpha phase c_p and k temperature dependence.

Figure 6 summarizes the prediction of temperature distribution sensitivity to c_p uncertainty in the time interval $451 \leq t \leq 551$ sec, which encompasses alpha phase existence. Throughout, the topmost graph presents the phase distribution, followed by the predicted temperature solution sensitivity to level, slope, and curvature of c_p temperature dependence. The corresponding units for the graphed sensitivities are $\text{K}^2\text{kg}/\text{J}$, $\text{K}^3\text{kg}/\text{J}$, and $\text{K}^4\text{kg}/\text{J}$, or more directly K/c_p , K^2/c_p , and K^3/c_p , where K denotes degrees Kelvin. Solution sensitivity to c_p level is very modest throughout with derivatives focused at the mold-casting and beta-alpha interfaces as expected.

Figure 7 presents the determined temperature solution sensitivity distributions to k uncertainty in the time interval $401 \leq t \leq 551$ sec. The direct units for these data are K/k , K^2/k , and K^3/k . The sensitivity to k uncertainties are an order more significant than to c_p uncertainties for the entire time frame, with a rather sharp extrema occurring at the beta-alpha interface.

The algorithm final prediction is displacement sensitivity to the c_p and k temperature dependence uncertainty throughout the casting-mold solidification history. Figures 8 and 9 summarize the predicted c_p and k uncertainty displacement sensitivities during the time interval $401 \leq t \leq 551$ sec. The direct units for these data are $\text{m}^2\text{kg}/\text{fs}$, $\text{m}^2\text{kgK}/\text{fs}$, and $\text{m}^2\text{kgK}^2/\text{fs}$, where $f = c_p, k$ respectively. The displacement sensitivities to c_p level, temperature-gradient, and temperature-gradient dependence are again muted in comparison to that predicted for k , and the significant digit for all variables is substantial in comparison to temperature sensitivity, Figures 6–7. Most noteworthy is the very sharp extrema occurring in k -sensitivity at the beta-alpha interface.

Table 1. Model problem thermo-physical material properties⁹

Representative Alloy				
Property	Liquid phase	Gamma phase	Beta phase	Alpha phase
ρ , kg/m ³	17250	17910	18130	19050
c_p , J/kgK	160 (assumed)	160	179	$103.6 + 0.0180 \cdot T + 8.49 \cdot 10^{-5} \cdot T^2$
k , W/mk	46.3 (assumed)	46.3	43.9	$8.6605 + 0.0488 \cdot T + 1.399 \cdot 10^{-5} \cdot T^2$
α , $\mu\text{m/mK}$	20 (assumed)	20	28	$4.06 + 0.0266 \cdot T$
Additional properties				
Melting temp., K	1406			
Phase change temp., K	mushy zone $\rightarrow \gamma$ (assumed) $\gamma \rightarrow \beta$ $\beta \rightarrow \alpha$			1350 1042 934
E, kg/m ²	$0.203 \cdot 10^{12}$			
ν	0.22			

IV. Conclusion

A casting solidification sensitivity theory focused on thermo-physical data temperature-dependence uncertainty has been developed. Identified thermo-physical data handling inconsistencies reported in the literature have been eliminated via this explicitly non-linear theory, producing exacting accuracy in handling material property uncertainty. As opposed to an inverse sensitivity analysis, with its attendant ill-posedness issues, a sequence of forward sensitivity simulation analyses can generate firm quantification of thermal displacement sensitivity to identified uncertainties. A computational simulation experiment for an axisymmetric casting of a generic alloy in a carbon mold has quantified algorithm performance.

Appendix

Following is the formulation of the finite element algorithm for the sensitivity algorithm applied in polar coordinates. The virtual work expression Π for an axisymmetric geometry is

$$\begin{aligned} \Pi = & \frac{1}{2} \int \{\epsilon_{rr}, \epsilon_{\theta\theta}\} \begin{bmatrix} 2G + \lambda & \lambda \\ \lambda & 2G + \lambda \end{bmatrix} \{\epsilon_{rr}, \epsilon_{\theta\theta}\}^T r dr d\theta \\ & - (3\lambda + 2G) \int \{\epsilon_{rr}, \epsilon_{\theta\theta}\} \begin{bmatrix} \alpha & 0 \\ 0 & \alpha \end{bmatrix} \{T\} r dr d\theta \end{aligned} \quad (\text{A.1})$$

Forming the displacement temperature sensitivity requires the derivative with respect to temperature, hence

$$\frac{\partial \Pi}{\partial T} = -\alpha(3\lambda + 2G) \int_{\Omega} \begin{bmatrix} \epsilon_{rr} & 0 \\ 0 & \epsilon_{\theta\theta} \end{bmatrix} r dr d\theta \quad (\text{A.2})$$

The next step is to form the FE algorithms for the radial displacement state $u(r)$ and the time-evolution of the temperature $T(r, t)$. The virtual work functional appropriate to this geometry involves both radial and azimuthal stress and strain contributions, combined with elastic Hooke's law. The kinematic strain-displacement relationship with FE implementation on the generic finite element domain is

$$\begin{aligned}
\begin{Bmatrix} \varepsilon_{rr} \\ \varepsilon_{\theta\theta} \end{Bmatrix} &= \begin{bmatrix} \partial/\partial r & 0 \\ 1/r & 0 \end{bmatrix} \begin{Bmatrix} u \\ 0 \end{Bmatrix} = \begin{Bmatrix} \partial/\partial r \\ 1/r \end{Bmatrix} u \\
&= \begin{Bmatrix} \partial/\partial r \\ 1/r \end{Bmatrix} \{N\}^T \{U\}_e = [\mathbf{D}] \{U\}_e
\end{aligned} \tag{A.3}$$

where $\{U\}_e$ is the nodal displacement array.

Evaluating Eq (A.2) as the sum of integrals formed on the radial discretization of the problem statement domain and substituting Eq (A.3) therein leads to evaluation of numerous integrals. The net result is construction of the [STIFF] and [THERM] matrices, as theory identified in Eq (8), on the generic FE domain. The forms are

$$[\text{STIFF}(\lambda, G)]_e = 2\pi \begin{bmatrix} (2G + \lambda) \left(\frac{\bar{R}_e}{\ell_e} + \frac{\ell_e}{3\bar{R}_e} \right) - \lambda & , & (2G + \lambda) \left(\frac{\bar{R}_e}{\ell_e} + \frac{\ell_e}{6\bar{R}_e} \right) - \lambda \\ (sym) & , & (2G + \lambda) \left(\frac{\bar{R}_e}{\ell_e} + \frac{\ell_e}{3\bar{R}_e} \right) - \lambda \end{bmatrix} \tag{A.4}$$

$$[\text{THERM}(\lambda, G, \alpha)]_e = -\alpha 2\pi (3\lambda + 2G) \begin{bmatrix} -\frac{1}{6} \{2, 1\} \{R\}_e + \frac{\ell_e}{3} & , & -\frac{1}{6} \{1, 2\} \{R\}_e + \frac{\ell_e}{3} \\ \frac{1}{6} \{2, 1\} \{R\}_e + \frac{\ell_e}{3} & , & \frac{1}{6} \{1, 2\} \{R\}_e + \frac{\ell_e}{3} \end{bmatrix} \tag{A.5}$$

In Eqs. (A.4)–(A.5), \bar{R}_e is element average radius, $\{R\}_e$ is element nodal radii, and ℓ_e is element length.

In summary, this FE thermal displacement computational theory, for displacement sensitivities determination including functional dependencies, is

$$\begin{aligned}
\Pi_{\text{ext}}^h &= S_e \{WS\}_e = \{0\} \\
\{WS\}_e &= [\text{STIFF}]_e \{U\}_e + [\text{THERM}]_e \{\text{TDIFF}\}_e \\
\text{where } [\text{STIFF}]_e, [\text{THERM}]_e &= [f_s(G, \lambda, \alpha, \bar{R}_e, \Omega^h)] \\
\{U\}_e &= \{UL, UR\}_e^T = \{\text{nodal radial displacement}\} \\
\{\text{TDIFF}\}_e &= \{\text{TDL, TDR}\}_e^T = \{\text{nodal relative temperature difference}\}
\end{aligned} \tag{A.6}$$

Construction of the FE algorithm for temperature evolution involves forming a Galerkin weak statement, embedded into a time Taylor series,⁵ yielding a non-linear algebraic equation system for the developed material property sensitivities. This system is assembled from element components $\{WS\}_e$, as in the structural model. An object-oriented template nomenclature for contributions admits full delineation of the detail, including the defined quadratic temperature dependence for specific heat and thermal conductivity via

$$\{WS\}_e \equiv (\text{const})(\text{avg})_e \{\text{dist}\}_e (\text{metric}) [\text{FE matrix}] \{Q \text{ or data}\}_e \tag{A.7}$$

The evaluation of WS_e contributions⁵ leads to the following template statements

$$\begin{aligned}
\{WS(c_p)\}_e &= (2\pi)(\text{ac}\bar{\rho}(\phi)) \{R\} (1) [\text{A3000}] \{Q - QN\}_e \\
&+ (2\pi)(\text{bc}\bar{\rho}, \bar{R}) \{Q\} (1) [\text{A3000}] \{Q - QN\}_e \\
&+ (2\pi)(\text{cc}\bar{\rho}, \bar{R}) \{Q, Q\} (1) [\text{A3000}] \{Q - QN\}_e
\end{aligned} \tag{A.8}$$

$$\begin{aligned}
\{WS(k)\}_e &= (2\pi)(\text{ak}) \{R\} (-1) [\text{A3011}] \{Q\} \\
&+ (2\pi)(\text{bk}, \bar{R}) \{Q\} (-1) [\text{A3011}] \{Q\} \\
&+ (2\pi)(\text{ck}, \bar{R}) \{Q, Q\} (-1) [\text{A3011}] \{Q\}
\end{aligned} \tag{A.9}$$

In these expressions, the temperature dependency coefficient sets {a,b,c} are also phase (ϕ) dependent, hence are element average data. Further, $\{Q\}$ denotes nodal temperature, $\{QN\}$ is nodal temperature from the previous time station solution, \bar{R} is the element average radius, and the 2π will eventually cancel out. The FE algorithm $\{WS\}_e$ template for radiation and thermal convection boundary conditions, for $\{QR\}$ and $\{QC\}$ the respective radiation and convection heat exchange temperatures on radial surface RR, RC, is

$$\begin{aligned} \{WS(\sigma, h)\}_e &= (2\pi, RR, \alpha\sigma) \{ \} \{ \} (0) [ONE] \{Qexp4\} \\ &+ (-2\pi, RR, \alpha\sigma) \{ \} \{ \} (0) [ONE] \{QRexp4\} \\ &+ (2\pi, RC, h) \{ \} \{ \} (0) [ONE] \{Q\} \\ &+ (-2\pi, RC, h) \{ \} \{ \} (0) [ONE] \{QC\} \end{aligned} \quad (A.10)$$

where the [ONE] matrix loads the expression at the appropriate boundary node.

The final temperature algorithm formation challenge is the form of latent heat release in the solidification mushy zone. Figure A.1 illustrates the assumed Hermite cubic functional form for f in the temperature interval ΔT between liquidus and gamma phase solidus temperatures T_l and T_γ . Proceeding through the numerous calculus details and defining the “potential” temperature in the mushy zone as $\Theta = (T - T_\gamma) / (T_l - T_\gamma)$, for L the latent heat, the cubically non-linear $\{WS\}_e$ template construction is

$$\begin{aligned} \{WS(L)\}_e &= (2\pi, 3, L) \{ \} \{R, \Theta\} (1) [A3000] \{\Theta\} \\ &+ (-2\pi, 2, L) \{ \} \{R, \Theta\} (1) [A3000] \{\Theta, \Theta\} \end{aligned} \quad (A.11)$$

Acknowledgments

The CFD Laboratory of the University of Tennessee, Knoxville performed this project under support from the Y-12 National Security Complex, Oak Ridge, Tennessee, Contract 4300017133.

Disclaimer

This work of authorship and those incorporated herein were prepared by the contractor as accounts of work sponsored by an agency of the United States Government. Neither the United States Government nor any agency thereof, nor Contractor, nor any of their employees, makes any warranty, express or implied, or assumes any legal liability or responsibility for the accuracy, completeness, use made, or usefulness of any information, apparatus, product, or process disclosed, or represents that its use would not infringe privately owned rights. Reference herein to any specific commercial product, process, or service by trade name, trademark, manufacturer, or otherwise, does not necessarily constitute or imply its endorsement, recommendation, or favoring by the United States Government or any agency or Contractor thereof. The views and opinions of authors expressed herein do not necessarily state or reflect those of the United States Government or any agency or Contractor thereof.

Copyright Notice

This document has been authored by a subcontractor of the U.S. Government under contract DE-AC05-00OR22800. Accordingly, the U.S. Government retains a paid-up, nonexclusive, irrevocable, worldwide license to publish or reproduce the published form of this contribution, prepare derivative works, distribute copies to the public, and perform publicly and display publicly, or allow others to do so, for U.S. Government purposes.

Figure Captions

- Figure 1. Sensitivity–uncertainty analysis organization.
- Figure 2. Casting model, liquid alloy in carbon mold.
- Figure 3. Truchas simulation solution, $t = 300$ sec.
- Figure 4. Sensitivity theory implementation axisymmetric geometry.
- Figure 5. Phase with displacement and temperature distributions during mold cooldown at (a) $t = 1$ sec, (b) $t = 51$ sec, (c) $t = 501$ sec.
- Figure 6. Phase with temperature distribution sensitivity to c_p uncertainty, kgK^2/J , level, slope, and curvature at (a) $t = 451$ sec, (b) $t = 501$ sec, (c) $t = 551$ sec.
- Figure 7. Phase with temperature distribution sensitivity to k uncertainty, mK^2/W , level, slope, and curvature at (a) $t = 401$ sec, (b) $t = 451$ sec, (c) $t = 501$ sec.
- Figure 8. Phase with displacement distribution sensitivity to c_p uncertainty, mkgK/J , level, slope, and curvature at (a) $t = 401$ sec, (b) $t = 451$ sec, (c) $t = 501$ sec, (d) $t = 551$ sec.
- Figure 9. Phase with displacement distribution sensitivity to k uncertainty, $\text{m}^2\text{K}/\text{W}$, level, slope, and curvature at (a) $t = 401$ sec, (b) $t = 451$ sec, (c) $t = 501$ sec, (d) $t = 551$ sec.
- Figure A.1. Hermite cubic distribution for latent heat release model.

References

- ¹D. Pelletier, J. Borggaard, and J. F. Hetu: “A Continuous Sensitivity Equation Method for Conduction and Phase Change Problems,” AIAA-2000-881, presented at 38th Aerospace Sciences Meeting and Exhibit, Reno, Nevada, Jan. 10-13, 2000.
- ²E. Turgeon, D. Pelletier, and J. Borggaard: “Sensitivity and Uncertainty Analysis for Variable Property Flows,” AIAA-2001-139, presented at 39th Aerospace Sciences Meeting and Exhibit, Reno, Nevada, Jan. 8-11, 2001.
- ³J. Borggaard, D. Pelletier and C. Winter: “Second-Order Sensitivity Analysis for Conjugate Phase-Change Problems,” AIAA-2003-512, presented at 41st Aerospace Sciences Meeting and Exhibit, Reno, Nevada, Jan. 6-9, 2003.
- ⁴A. J. Baker, J. L. Frankel, K. L. Wong, M. A. Grubert, and V. E. Lamberti: *Inverse Uncertainty-Sensitivity Analyses for Heavy Metal Casting Simulation Applications*, Final Technical Report, Contract 4300017133, Y-12 National Security Complex, Oak Ridge, Tennessee, September 2003.
- ⁵A. J. Baker: *Finite Element Problem Solving Environment*, UT CFD Lab Press, Knoxville, 2004.
- ⁶I. H. Shames and C. L. Dym: *Energy and Finite Element Methods in Structural Mechanics*, Mc Graw-Hill, New York, 1985.
- ⁷TRUCHAS, Software Package, Los Alamos National Laboratory, Los Alamos, New Mexico.
- ⁸MATLAB, Computational Engineering Toolbox, Software Package, Ver. 13, The MathWorks, Natick, Massachusetts.
- ⁹*American Society for Metals Handbook*, 10th ed., vol. 2, pp. 1197-8.

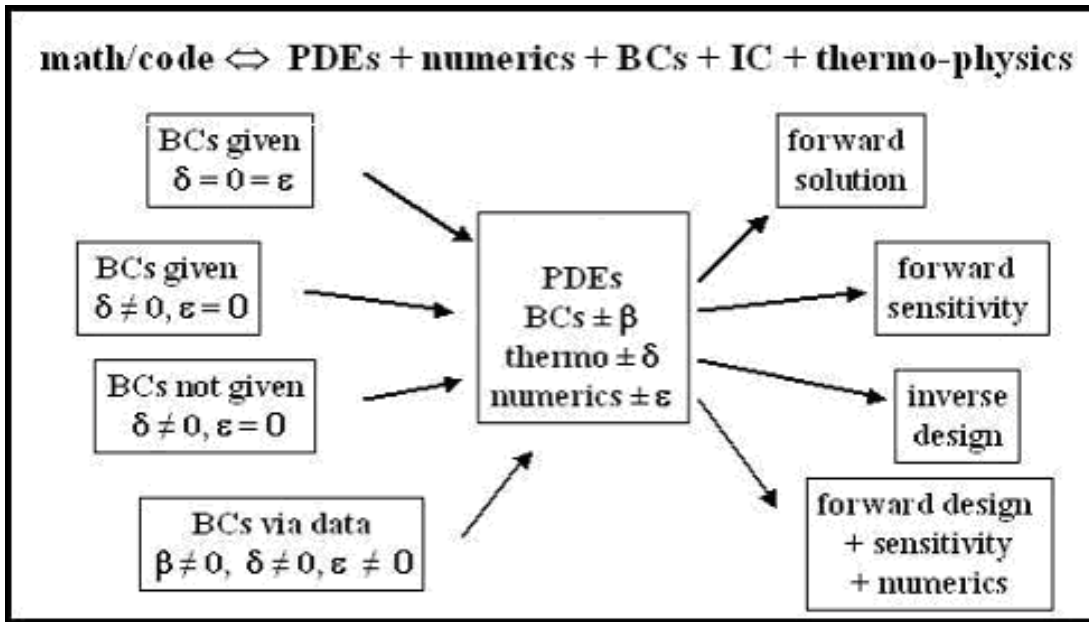


Figure 1. Sensitivity-uncertainty analysis organization.

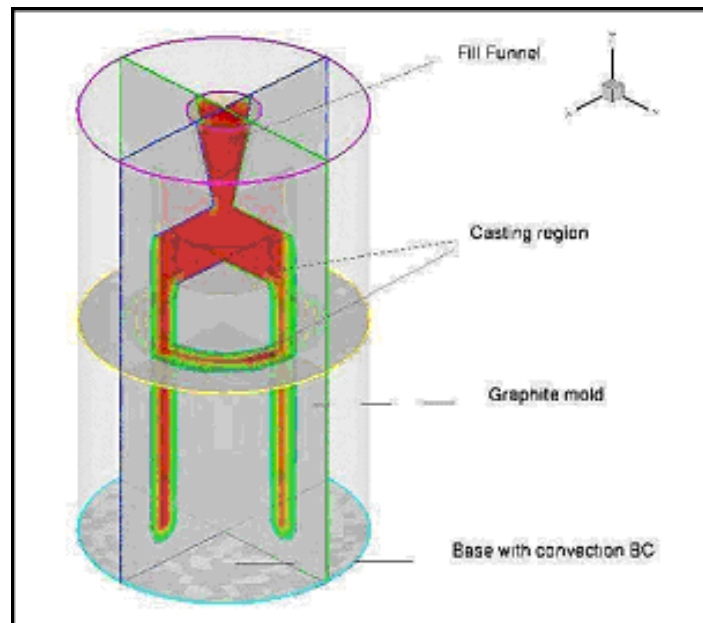


Figure 2. Casting model, liquid alloy in carbon mold.

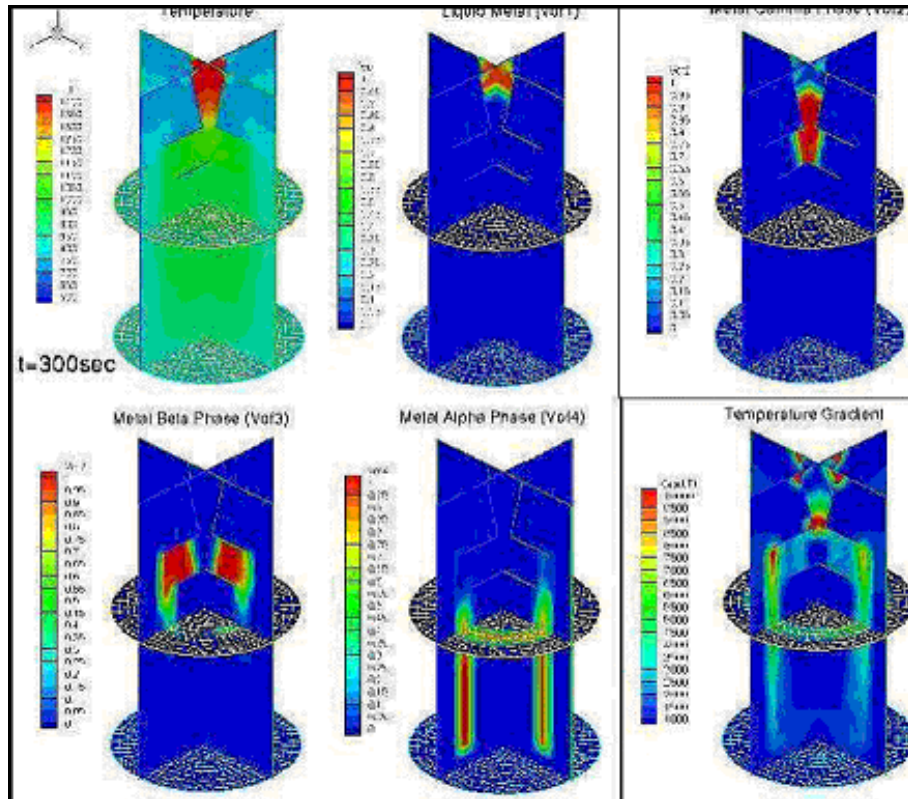


Figure 3. Truchas simulation solution, $t = 300$ sec.

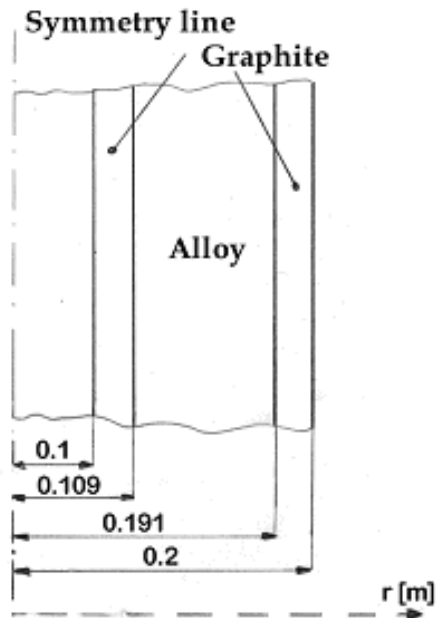


Figure 4. Sensitivity theory implementation axisymmetric geometry.

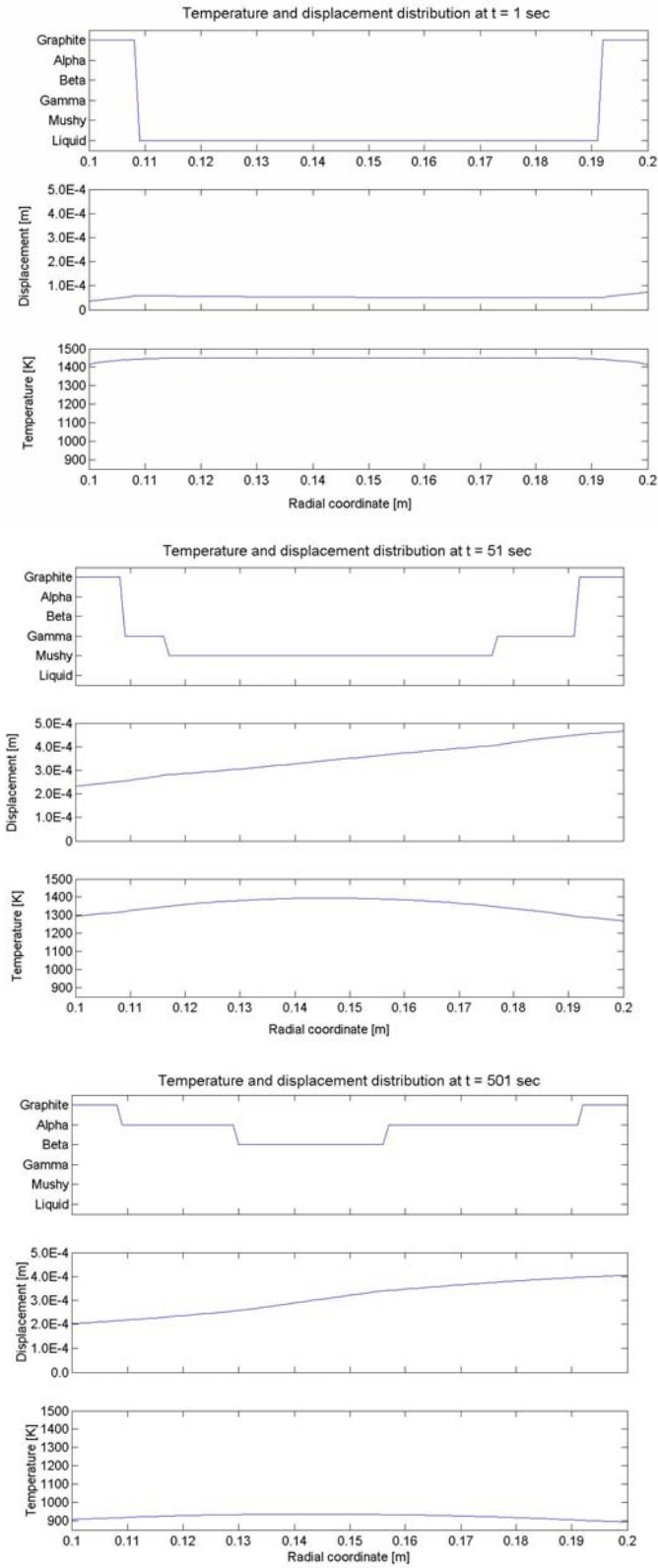


Figure 5. Phase with displacement and temperature distributions during mold cool-down at (a) t = 1 sec, (b) t = 51 sec, (c) t = 501 sec.

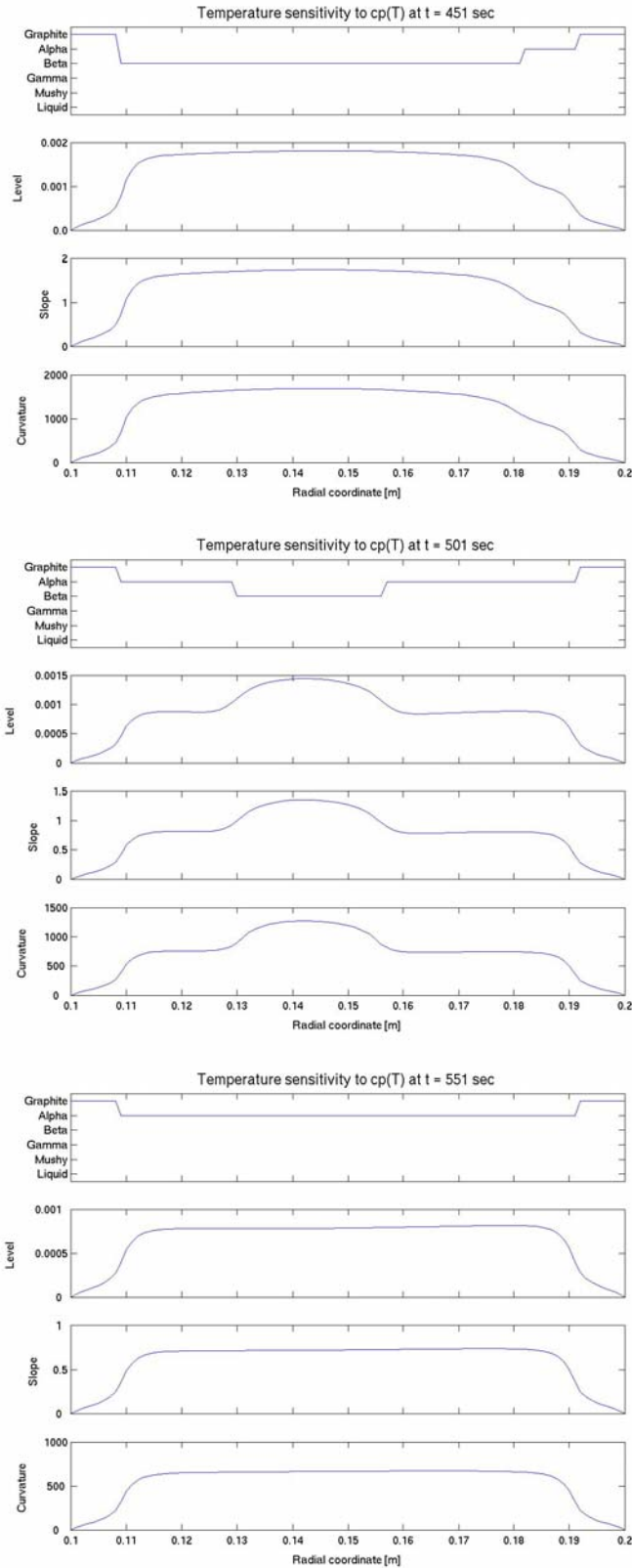


Figure 6. Phase with temperature distribution sensitivity to c_p uncertainty, kgK^2/J , level, slope, and curvature at (a) $t = 451$ sec, (b) $t = 501$ sec, (c) $t = 551$ sec.

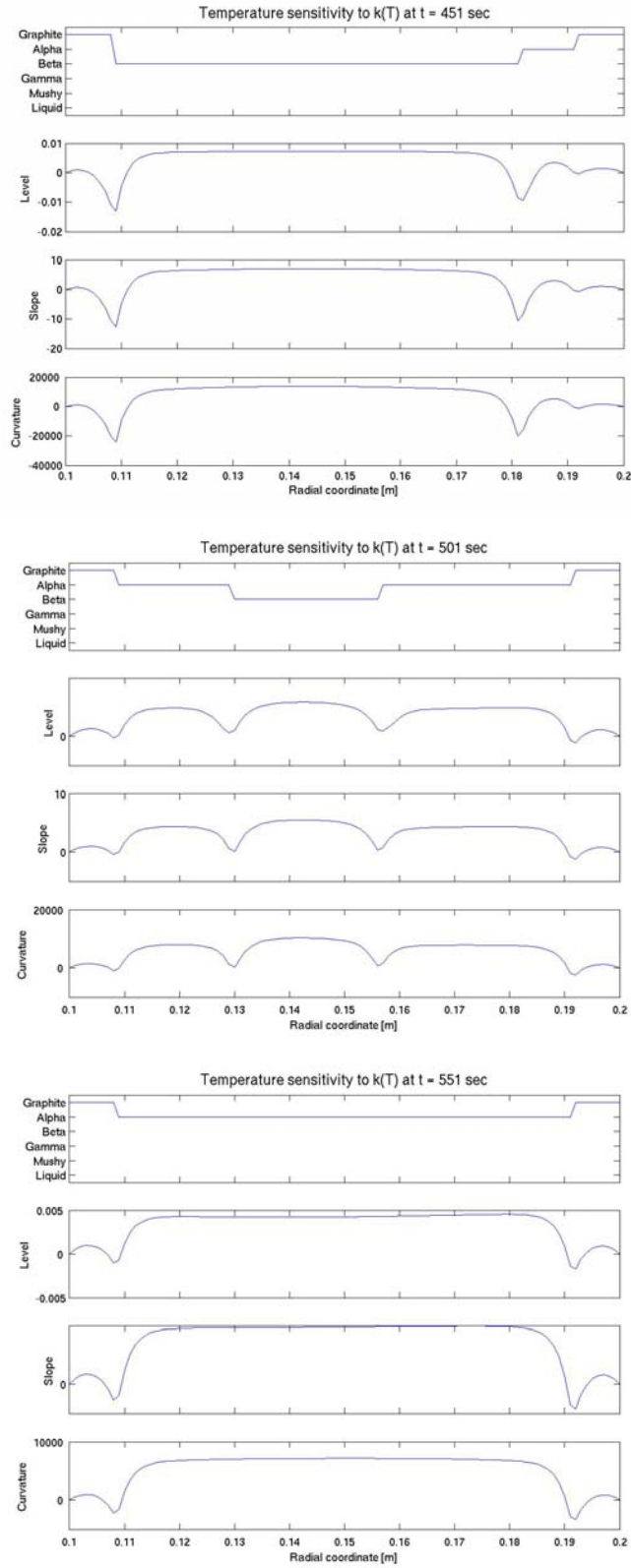
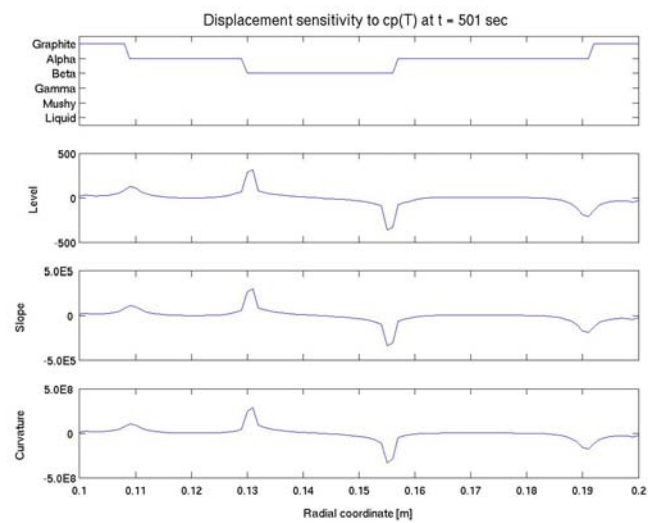
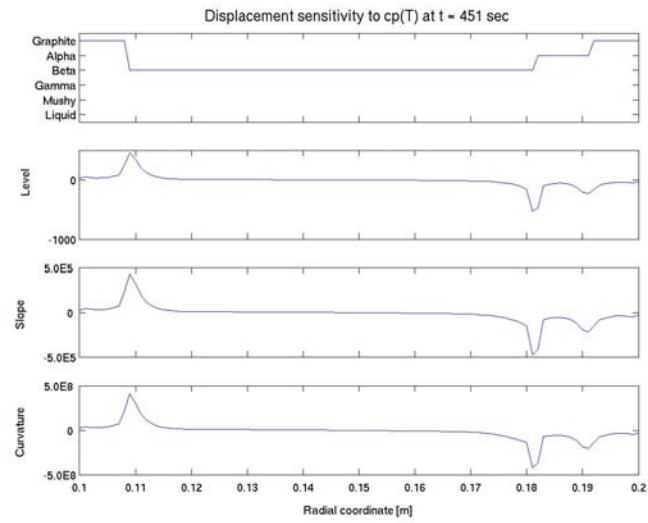
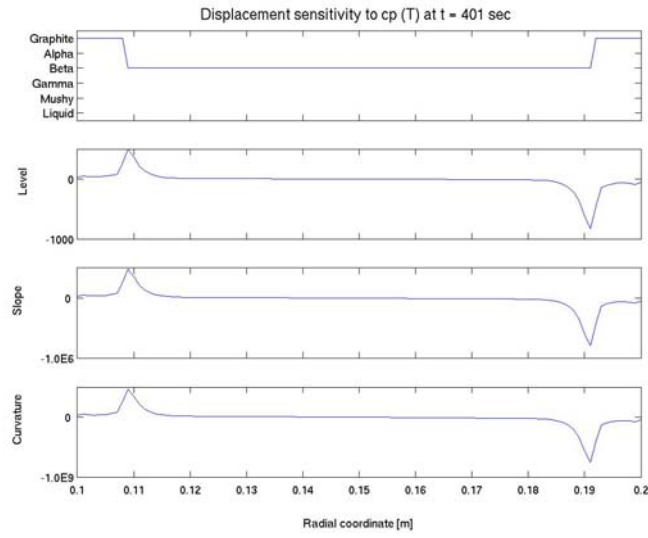


Figure 7. Phase with temperature distribution sensitivity to k uncertainty, mK^2/W , level, slope, and curvature at (a) $t = 401$ sec, (b) $t = 451$ sec, (c) $t = 501$ sec.



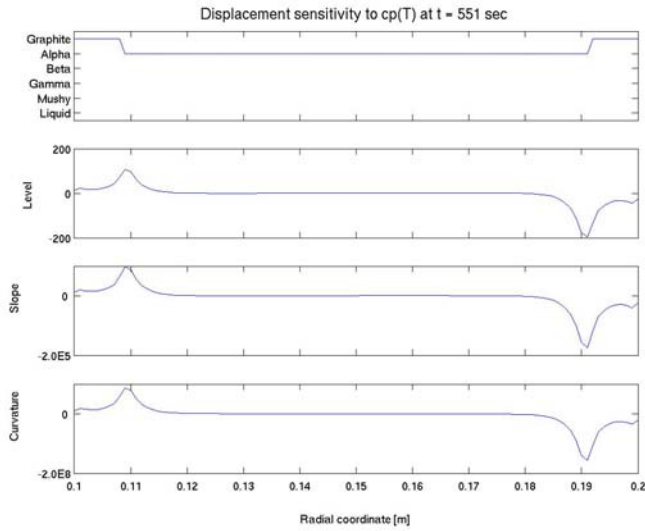
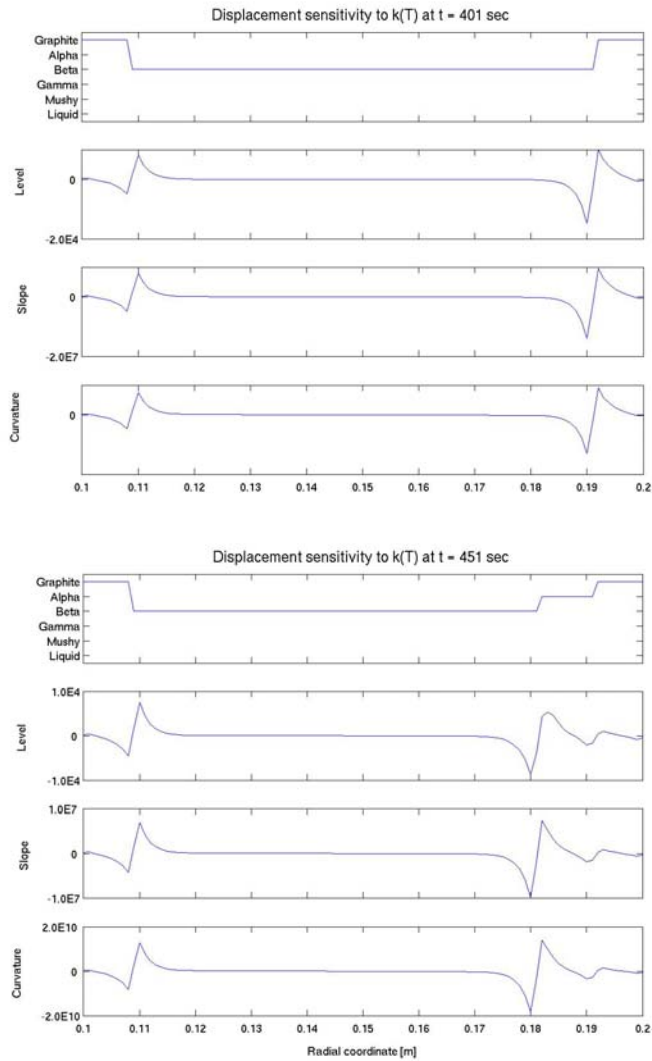


Figure 8. Phase with displacement distribution sensitivity to c_p uncertainty, mkgK/J , level, slope, and curvature at (a) $t = 401$ sec, (b) $t = 451$ sec, (c) $t = 501$ sec, (d) $t = 551$ sec.



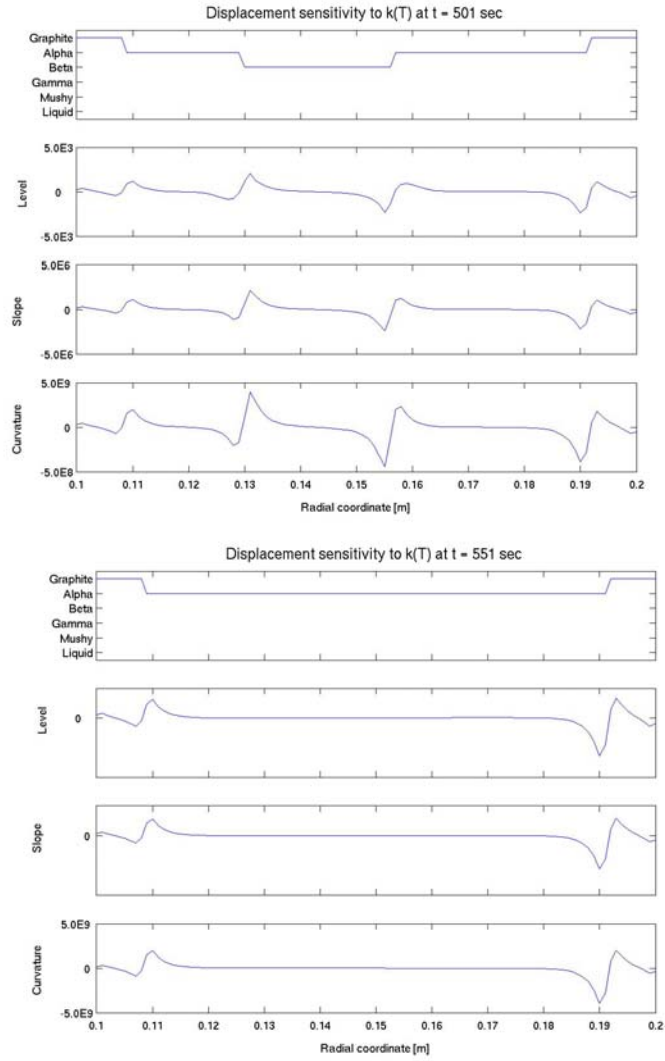


Figure 9. Phase with displacement distribution sensitivity to k uncertainty, m^2K/W , level, slope, and curvature at (a) $t = 401$ sec, (b) $t = 451$ sec, (c) $t = 501$ sec, (d) $t = 551$ sec.

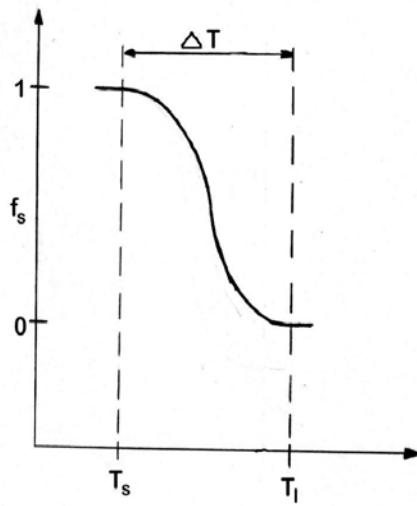


Figure A.1. Hermite cubic distribution for latent heat release model.